Peer-reviewed version available at Magnetochemistry 2018, 4, 27; doi:10.3390/magnetochemistry4020027

Theory of Electron Spin Resonance in Ferromagnetically Correlated Heavy Fermion Compounds

P. Schlottmann[1,2]

[1] *Department of Physics, Florida State University, Tallahassee, Florida 32306, USA*

[2] *Correspondence: E-mail: pschlottmann@fsu.edu; Tel.: (850) 644-0055*

Abstract

We study the electron spin resonance (ESR) line width for localized moments within the framework of the Kondo lattice model. An ESR signal for an impurity can only be observed if the Kondo temperature is sufficiently small. On the other hand, for the Kondo lattice, short-range ferromagnetic correlations (FM) between the localized spins are necessary to obtain an observable signal. The spin relaxation rate (line width) is inversely proportional to the static magnetic susceptibility. The FM enhance the susceptibility and hence reduce the line width. For most of the heavy fermion systems displaying an ESR signal the FM arise in the *ab*-plane from the strong lattice anisotropy.

An ESR signal was observed in the *cubic* heavy fermion compound CeB_6 which has a Γ_8 ground-quartet. The orbital content of the Γ_8-quartet gives rise to an antiferro-quadrupolar ordered (AFQ) phase below 4 K. Single ions with a Γ_8 ground-multiplet are expected to display four transitions, however, only one has been observed. We address the effects of the interplay of AFQ and FM on the phase diagram and the ESR line width. While for anisotropic Ce and Yb compounds with ESR-signal it is difficult to distinguish if the resonance is due to localized spins or conducting heavy electron spins, an itinerant picture within the AFQ phase is necessary to explain the electron spin resonances for CeB_6.

The longitudinal magnetic susceptibility has a quasi-elastic central peak of line width $1/T_1$ and inelastic peaks for the absorption/emission of excitation. The latter are measured via inelastic neutron scattering (INS) and provide insights into the magnetic order. We briefly summarize some of the INS results for CeB_6 in the context of the picture that emerged from the ESR experiments.

Keywords: Kondo lattice, localized moments, ferromagnetic correlations

PACS numbers: 72.15.Qm, 76.30.-v, 75.20.Hr, 71.27.+a

I. INTRODUCTION

The Kondo effect is the compensation into a singlet state of an impurity spin-1/2 by the spin density of the conduction electrons. As a consequence the impurity spin S is no longer a good quantum number and the magnetic susceptibility χ_0 and the spin-relaxation time T_1 are finite. According to the Shiba relation[1,2] for $\omega = T = H = 0$, χ_0 and T_1 are proportional to each other ($\chi_0/T_1 = 2/\pi$) and inversely proportional to the characteristic energy, T_K, known as the Kondo temperature. Hence, an electron spin resonance (ESR) signal for a Kondo impurity cannot be observed unless T_K is smaller than 100 mK for X-band microwave frequencies.[3]

The above suggests that the ESR linewidth is too broad in heavy fermion compounds to be observed. This common belief was proven incorrect when an ESR signal was found in single crystals of $YbRh_2Si_2$,[4–6] $YbIr_2Si_2$,[7] YbRh,[8] $YbCo_2Zn_{20}$,[9], CeRuPO,[10], and CeB_6.[11,12] The resonances are attributed to the Yb^{3+} and Ce^{3+} ions despite of their rather large T_K. All these compounds have strong magnetic anisotropy (except for CeB_6) and ferromagnetic correlations among the rare earth spins.[8] The observed resonances have a Dysonian line shape,[13–15] as expected from the skin depth and spin diffusion in a metallic environment.

The ESR of local magnetic moments in a metal[16–18] as well as the resonance of conduction electrons have a similar Dysonian line shape[13–15] and are very difficult to distinguish. The analysis of the data performed within the known framework of ESR of magnetic impurities in metals,[16–18] i.e., single ions with localized spins resonating independently, is consistent with the g-factor anisotropy expected for a tetragonal crystalline electric field and a line width. It has been estimated that in $YbRh_2Si_2$ more than 60% of the Yb3+ ions contribute to be ESR signal.[7,19] On the other hand, in the case of a band of conducting heavy electrons, the g-shift is dominated by one of the f orbitals and is going to have the crystalline field anisotropies of the rare-earth sites. Based solely on ESR it is then difficult to decide if the resonances arise from localized moments or the carriers in a heavy-electron band.[20]

Abrahams and Wölfle[21] studied the line width of the ESR signal for a heavy fermion compound within the framework of the Anderson lattice. They obtained that the heavy mass in conjunction with ferromagnetic fluctuations can lead to observable narrow resonances. The heavy mass is equivalent with arguing with a small Kondo temperature for the lattice, but is not enough to produce an observable ESR signal. The ferromagnetic correlations

further reduce the linewidth of the signal. Wölfle and Abrahams[22] applied their theory to the Fermi liquid regime for $YbRh_2Si_2$ and found good agreement with the experimental data. They also extended the description to the non-Fermi liquid regime of this material and found a close relation of the T dependence of the specific heat and spin susceptibility with the observed T dependence of the g-shift and the linewidth.[23,24]

Schlottmann[20] arrived at similar results to those in Ref. [21] by studying the dynamical susceptibility for localized spins within the framework of the Kondo lattice instead of the Anderson lattice. Based on the proportionality of the linewidth with the inverse magnetic susceptibility this investigation clearly shows the relevance of the ferromagnetic correlations. The Kondo effect replaced the Curie-law with a Curie-Weiss law with an antiferromagnetic Weiss temperature slightly larger than the Kondo temperature. This would produce a broad ESR line and is hence not observable. Ferromagnetic long-range order, on the other hand, changes the sign of the Curie-Weiss temperature and hence enhances the susceptibility in the paramagnetic phase, giving rise to an observable resonance.

Several other approaches to explain the ESR in heavy fermion systems have been proposed. Zvyagin *et al.*[25] considered a system with strong local anisotropic electron-electron interactions and showed that together with a hybridization between localized and itinerant electrons it may cause a g-shift of the ESR signal and a change in the linewidth. Huber,[26] on the other hand, studied the effects of anisotropy and the Yb-Yb interactions on the low-field ESR in $YbRh_2Si_2$ and $YbIr_2Si_2$ with main emphasis on the anisotropy of the g-shift. Finally, for the anisotropic Kondo model with anisotropic Ruderman-Kittel-Kasuya-Yosida (RKKY) interaction, Kochelaev *et al.*[27] investigated the relaxation of a collective spin mode assuming that the Kondo coupling has the same anisotropy as the g-factor.

The remainder of the paper is organized as follows. In sect. II we introduce the Kondo lattice model and the transverse dynamical susceptibility. In sect. III the dynamical susceptibility is explicitly calculated in terms of a relaxation function using second order perturbation theory in the exchange coupling. Single site terms and inter-site contributions are treated separately. In sect. IV we discuss the consequences for impurities and for the lattice considering a paramagnetic host, an antiferromagnetic lattice and ferromagnetic correlations. In sect. V we summarize our results for the cubic system CeB_6. In this compound the Ce^{3+} ions have a Γ_8-quartet ground state, allowing for a richer spectrum of resonances. In sect. VI we study the longitudinal dynamical susceptibility, which yields the spin-flip

relaxation time and is of relevance for neutron scattering. Finally, conclusions follow in sect. VII.

II. THE KONDO LATTICE MODEL AND THE TRANSVERSAL DYNAMICAL SUSCEPTIBILITY

The Kondo lattice consists of the kinetic energy of the conduction electrons and a spin $S = 1/2$ at every lattice site interacting via spin exchange J with the conduction states, i.e. $\mathcal{H} = \mathcal{H}_0 + \mathcal{H}_{sd}$, with

$$\begin{aligned} H_0 &= \sum_{\mathbf{k}\sigma} \epsilon_{\mathbf{k}\sigma} c^\dagger_{\mathbf{k}\sigma} c_{\mathbf{k}\sigma} - g_f \mu_B B \sum_j S^z_j \ , \\ H_{sd} &= \frac{J}{N} \sum_{\mathbf{k}\mathbf{k}'\sigma\sigma' j} e^{i(\mathbf{k}-\mathbf{k}')\cdot\mathbf{R}_j} c^\dagger_{\mathbf{k}\sigma} \mathbf{S}_j \cdot \mathbf{s}_{\sigma\sigma'} c_{\mathbf{k}'\sigma'} \ . \end{aligned} \tag{1}$$

Here j labels the spin sites, $\mathbf{R}_j$ denotes the position of the site j, $\mathbf{S}_j$ are the spin-1/2 operators for the localized spin at site j and $\mathbf{s}_{\sigma\sigma'}$ denotes 1/2 times the Pauli matrices for the conduction states. $g_f \mu_B B$ is the Zeeman splitting. Similarly, for the conduction electrons we have $\epsilon_{\mathbf{k}\sigma} = \epsilon_{\mathbf{k}} - \sigma B_c/2$, where $B_c = g_c \mu_B B$. It is convenient to work with the Hartree-Fock factorization of H_{sd}, i.e. we replace

$$B \to B' = B - J\rho_F g_c \mu_B B/2 \ . \tag{2}$$

This corresponds to the "Knight-shift" of the magnetic resonance.

The ESR line is given by the transverse dynamical susceptibility. According to Eq. (1) the Zeeman field is along the z-direction and, hence, the microwave field rotates in the $x-y$ plane, i.e.

$$\chi^T(z) = -(g_f \mu_B)^2 \frac{1}{2N} \sum_{ij} \langle\langle S^+_i ; S^-_j \rangle\rangle_z \ , \tag{3}$$

where N is the number of rare earth sites, $S^\pm_j = S^x_j \pm i S^y_j$ are the spin-flip operators at site j, $z = \omega + i0$ is the external frequency, and the factor $1/2$ is introduced to normalize the susceptibility (note that the S^x and S^y correlation functions are equal). The spin operators satisfy the standard commutation relations, $[S^+_j, S^-_j] = 2S^z_j$ and $[S^z_j, S^\pm_j] = \pm S^\pm_j$, while spin operators of different sites commute with each other.

Applying equation of motion on the first argument of the susceptibility we obtain

$$\chi^T(z) = \frac{-(g_f \mu_B)^2 \langle S^z \rangle + \psi(z)}{z - g_f \mu_B B'} \ , \tag{4}$$

where $\langle S^z \rangle$ is the spin polarization per site and

$$\psi(z) = -(g_f\mu_B)^2 \frac{J}{2N^2} \sum_{\mathbf{k}\mathbf{k}'\sigma\sigma' ij} e^{i(\mathbf{k}-\mathbf{k}')\cdot\mathbf{R}_i} \langle\langle (-S_i^+ s_{\sigma\sigma'}^z + S_i^z s_{\sigma\sigma'}^+) c_{\mathbf{k}\sigma}^\dagger c_{\mathbf{k}'\sigma'}; S_j^- \rangle\rangle_z. \tag{5}$$

The equation of motion on the second argument yields

$$\begin{aligned}(z - g_f\mu_B B')\psi(z) \;=\; & -(g_f\mu_B)^2 \frac{J}{2N^2} \sum_{\mathbf{k}\mathbf{k}'\sigma\sigma' i} e^{i(\mathbf{k}-\mathbf{k}')\cdot\mathbf{R}_i} \left\{ -2\langle S_i^z s_{\sigma\sigma'}^z c_{\mathbf{k}\sigma}^\dagger c_{\mathbf{k}'\sigma'} \rangle - \langle S_i^- s_{\sigma\sigma'}^+ c_{\mathbf{k}\sigma}^\dagger c_{\mathbf{k}'\sigma'} \rangle \right\} \\ & + (g_f\mu_B)^2 \frac{J^2}{2N^3} \sum_{ij} \sum_{\mathbf{k}\mathbf{k}'\sigma\sigma'} \sum_{\mathbf{p}\mathbf{p}'\tau\tau'} e^{i(\mathbf{k}-\mathbf{k}')\cdot\mathbf{R}_i} e^{i(\mathbf{p}-\mathbf{p}')\cdot\mathbf{R}_j} \\ & \times \langle\langle (-S_i^+ s_{\sigma\sigma'}^z + S_i^z s_{\sigma\sigma'}^+) c_{\mathbf{k}\sigma}^\dagger c_{\mathbf{k}'\sigma'}; (S_j^- s_{\tau\tau'}^z - S_j^z s_{\tau\tau'}^+) c_{\mathbf{p}\tau}^\dagger c_{\mathbf{p}'\tau'} \rangle\rangle_z \;, \end{aligned} \tag{6}$$

which can be evaluated for the noninteracting system and rewritten as

$$\begin{aligned}(z - g_f\mu_B B')\psi(z) \;=\; & (g_f\mu_B)^2 \frac{J}{2N^2} \sum_{\mathbf{k}\mathbf{k}'\sigma\sigma' i} e^{i(\mathbf{k}-\mathbf{k}')\cdot\mathbf{R}_i} \left\{ 2\langle S_i^z s_{\sigma\sigma'}^z c_{\mathbf{k}\sigma}^\dagger c_{\mathbf{k}'\sigma'} \rangle + \langle S_i^- s_{\sigma\sigma'}^+ c_{\mathbf{k}\sigma}^\dagger c_{\mathbf{k}'\sigma'} \rangle \right\} \\ & - (g_f\mu_B)^2 \frac{J^2}{2N^3} \sum_{ij} \sum_{\mathbf{k}\mathbf{k}'} e^{i(\mathbf{k}-\mathbf{k}')\cdot\mathbf{R}_i - \mathbf{R}_j} \frac{f(\epsilon_{\mathbf{k}}) - f(\epsilon_{\mathbf{k}'})}{z - \epsilon_{\mathbf{k}'} + \epsilon_{\mathbf{k}}} \langle S_i^z S_j^z \rangle \\ & - (g_f\mu_B)^2 \frac{J^2}{4N^3} \sum_{ij} \sum_{\mathbf{k}\mathbf{k}'} e^{i(\mathbf{k}-\mathbf{k}')\cdot\mathbf{R}_i - \mathbf{R}_j} \frac{f(\epsilon_{\mathbf{k}}) - f(\epsilon_{\mathbf{k}'})}{z - \epsilon_{\mathbf{k}'} + \epsilon_{\mathbf{k}} - g_f\mu_B B'} \langle S_i^+ S_j^- \rangle \\ & - (g_f\mu_B)^2 \frac{J^2}{2N^3} \sum_{\mathbf{k}'i} \frac{f(\epsilon_{\mathbf{k}'})[1 - f(\epsilon_{\mathbf{k}})]}{z - \epsilon_{\mathbf{k}'} + \epsilon_{\mathbf{k}} - g_f\mu_B B'} \langle S_i^z \rangle \quad . \end{aligned} \tag{7}$$

Here $f(\epsilon_{\mathbf{k}})$ represents the Fermi distribution function and we have neglected the Zeeman field of the conduction electrons.

The dynamics of the magnetic moments is usually described by Bloch's equations,[28] which can be cast into the form[29,30]

$$\chi^T(z) = \left[z - B_{eff} + N^T(z)/\chi_0^T \right]^{-1} \left[-B_{eff}\chi_0^T + N^T(z) \right] \quad , \tag{8}$$

where $B_{eff} = g_f\mu_B B'$ is the effective Zeeman splitting and χ_0^T is the static transverse magnetic susceptibility. For the noninteracting system we have $\chi_0^T = (g_f\mu_B)^2 \langle S^z \rangle / B_{eff}$. $N^T(z)$ is called the relaxation function. Assuming that $N^T(z)$ is an imaginary constant at low frequencies, we can identify $N^T(0)$ with $i\chi_0^T/T_2$ and Eq. (8) reduces to a Lorentzian resonance shape. Comparing Eqs. (4) and (7) with Eq. (8) we obtain the relaxation function to second order in the exchange J, i.e.,[29]

$$(z - g_f\mu_B B')\chi^T(z) + g_f\mu_B B'\chi_0^T = \frac{1}{z - g_f\mu_B B'} z N^T(z) = \psi(z) \quad . \tag{9}$$

We are mainly interested in the imaginary part of $N^{T''}(\omega)$. The first term in (7) is real and does not contribute. For the remaining terms the angular integrals of momenta are carried out and the $(z-\epsilon_{\mathbf{k}'}+\epsilon_{\mathbf{k}})$ factors in the denominator are converted into δ-functions, so that for a parabolic band we obtain

$$N^{T''}(\omega)=\frac{\pi}{2N}(g_f\mu_B J\rho_F)^2\sum_{ij}\frac{\sin(k_F R_{ij})^2}{(k_F R_{ij})^2}\langle S_i^z S_j^z\rangle$$
$$+\frac{\pi}{4N}(g_f\mu_B J\rho_F)^2\frac{\omega-g_f\mu_B B'}{\omega}\sum_{ij}\frac{\sin(k_F R_{ij})^2}{(k_F R_{ij})^2}\left[\langle S_i^+ S_j^-\rangle+2\delta_{ij}\langle S_i^z\rangle\frac{1}{e^{(\omega-g_f\mu_B B')/T}-1}\right] \quad (10)$$

It is convenient to treat single site and multiple site terms separately. Using that $\langle S^z\rangle=(1/2)\tanh[(g_f\mu_B B')/(2T)]$ we obtain for the single site contribution

$$N_s^{T''}(\omega)=\frac{\pi}{4}(g_f\mu_B J\rho_F)^2\left\{\frac{1}{2}+\langle S^z\rangle\frac{\omega-g_f\mu_B B'}{\omega}\left[\coth\left(\frac{\omega-g_f\mu_B B'}{2T}\right)+\coth\left(\frac{g_f\mu_B B'}{2T}\right)\right]\right\}, \quad (11)$$

which agrees with the result of Ref. 29, and for the multi-site terms

$$N_m^{T''}(\omega)=\frac{\pi}{4N}(g_f\mu_B J\rho_F)^2\sum_{ij,i\neq j}\frac{\sin(k_F R_{ij})^2}{(k_F R_{ij})^2}e^{-R_{ij}/l}\left[2\langle S_i^z S_j^z\rangle+\frac{\omega-g_f\mu_B B'}{\omega}\langle S_i^+ S_j^-\rangle\right], \quad (12)$$

where l is the spin mean-free path due to the spin-lattice relaxation. Our spin S is actually a pseudo-spin arising from the crystalline field splittings of the rare earth total angular momentum. As such it has a large orbital component due to the strong spin-orbit interaction. When the conduction electrons travel, their "spin" relaxes into the lattice (spin-lattice relaxation).

The resonance takes place at the field B' and the spin relaxation rate is now given by

$$\frac{1}{T_2}=\frac{N^{T''}(\omega=B')}{\chi_0^T}\ , \quad (13)$$

where $N^{T''}=N_s^{T''}+N_m^{T''}$.

III. SPECIAL CASES

In this section we discuss the consequences of the single site and multiple site contributions for different magnetic orders of the host.

A. Korringa relaxation

For the isolated impurity case we consider only the single site terms. The single site relaxation function $N_s^{T''}(\omega)$ can be regularized into an analytic function[29]

$$\begin{aligned} N^T(z) &= (g_f\mu_B)^2\frac{\pi}{4}(J\rho_F)^2\Big[i+\frac{2}{\pi}\langle S^z\rangle\phi(z)\Big] \\ \phi(z) &= \ln(D/2\pi T)-\frac{z-g_f\mu_B B'}{z}\psi\Big(1-i\frac{z-g_f\mu_B B'}{2\pi T}\Big)-\frac{g_f\mu_B B'}{z}\psi\Big(1+i\frac{g_f\mu_B B'}{2\pi T}\Big) \end{aligned} \quad (14)$$

where ψ is the digamma function and D is the band cut-off. This is the exact expression to second order in J of the relaxation function.

Using $z=\omega+i0$ we may now expand the function $N^T(z)$ for small $(\omega-g_f\mu_B B')$ as $N^T(z)=\Delta'+i\Delta''+(\gamma'+i\gamma'')(\omega-g_f\mu_B B')+\cdots$. The dynamical susceptibility has then a Lorentzian shape with a relaxation rate[29]

$$1/T_{rel}=\Delta''/(\chi_0^T+\gamma')\ , \quad (15)$$

where

$$\begin{aligned} \Delta'' &= (g_f\mu_B)^2\frac{\pi}{4}(J\rho_F)^2\Big[i+\frac{2}{\pi}\langle S^z\rangle\mathrm{Im}\psi\Big(1+i\frac{g_f\mu_B B'}{2\pi T}\Big)\Big]\ , \\ \gamma' &= (g_f\mu_B)^2\frac{\pi}{4}(J\rho_F)^2\frac{2}{\pi}\frac{\langle S^z\rangle}{g_f\mu_B B'}\mathrm{Re}\left[\psi\Big(1+i\frac{g_f\mu_B B'}{2\pi T}\Big)-\psi(1)\right]\ , \end{aligned} \quad (16)$$

and Im and Re denote imaginary and real part, respectively. Here γ' contains the retardation effects due to the frequency dependence of $N^T(z)$. To obtain the relaxation rate to second order in J, we only need the free ion $\langle S^z\rangle=(1/2)\tanh(g_f\mu_B B'/2T)$ and $\chi_0^T=\langle S^z\rangle/(g_f\mu_B B')$.[29]

In the limit $B'\to 0$ we obtain

$$\frac{1}{T_{rel}}=\pi(J\rho_F)^2T\ , \quad (17)$$

which is the well-established Korringa relaxation rate. This relaxation rate is proportional to T. Here the factor T arises from the inverse of χ_0^T, while, alternatively and equivalently, in textbook calculations the T originates from the integration over the Fermi functions for the conduction electrons.

If, on the other hand, $g_f\mu_B B' >> T$ the result is

$$\frac{1}{T_{rel}}=\frac{\pi}{4}(J\rho_F)^2\frac{g_f\mu_B B'}{1+\frac{1}{2}(J\rho_F)^2\ln(g_f\mu_B B'/2\pi T)}\ , \quad (18)$$

so that the line width increases almost linearly with the external field. Hence, at low T the residual line width in X-band ESR should be less than the corresponding one for Q-band, as found in many experiments.

B. The Kondo impurity

So far we considered second order perturbation theory in J. Terms of higher order in J introduce the Kondo effect. The Kondo effect affects both the relaxation function $N^T(z)$ and the static susceptibility χ_0^T.

For the case $T \gg T_K$ the Kondo terms appear as logarithmic corrections as a consequence of dressing the interaction vertex. The renormalized vertex introduces an enhancement (on a logarithmic scale) to $N^T(z)$.[31,32] Also χ_0^T acquires logarithmic corrections reducing the suceptibility. Both effects are the precursor of the compensation of the localized spin at low temperatures and fields by the spin-density of the conduction electrons. At high T the relaxation rate resembles a Korringa behavior, i.e. linear in T, with an enhanced exchange coupling and logarithmic corrections. The relaxation rate is approximately given by

$$\frac{1}{T_2} = \frac{\pi}{2} T \left[1 + \frac{(g_f \mu_B B'/2T)}{\tanh(g_f \mu_B B'/2T)}\right] \left[\ln(T/T_K) + \frac{1}{2}\psi(1) + \frac{1}{2}\mathrm{Re}\psi(1 - i g_f \mu_B B'/2\pi T)\right]^{-2} , \tag{19}$$

where ψ is the digamma function. The application of these results to ^{171}Yb and ^{174}Yb impurities in Au can be found in Ref. 3. The data for Au^{171}Yb are shown in Fig. 1 for a slightly different fit with $T_K = 0.5 \times 10^{-8}$ K. The Kondo logarithms are necessary for a reasonable agreement.

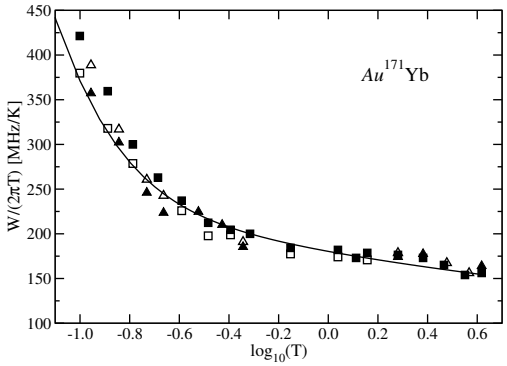

FIG. 1: Relaxation rate over T of Au^{171}Yb for 9 GHz (X-band) as a function of T. Open symbols denote the $m_I = +1/2$ transitions and closed symbols the $m_I = -1/2$ transitions. Triangles correspond to a sample with 280 ppm and squares to a sample with 670 ppm. The solid curve is Eq. 19 for $T_K = 0.5 \times 10^{-8}$ K. Adapted from Ref. 3.

For $|\omega|, T, g_f \mu_B B' \ll T_K$, on the other hand, a singlet spin state forms as a consequence

of the Abrikosov resonance. The susceptibility is finite (in contrast to the Curie law) and the relaxation function is determined by the unitarity bound for the Kondo scattering, i.e. $N^T(z = T = B' = 0) = i2(g_f\mu_B)^2/\pi$, giving rise to Fermi liquid properties. Note that as expected in this limit the relaxation function is independent of the exchange constant J.[1,2] As a function of ω and T, the imaginary part of N^T decreases as $(\omega/T_K)^2$ and $(T/T_K)^2$. The susceptibility χ_0^T is a constant (there are Van Vleck-like transitions from the singlet into the excited spin triplet) of the order of $1/T_K$. The relaxation rate is then of the order of T_K instead of being proportional to the temperature (Korringa), so that only if T_K is less than 100 mK it would possible to observe an X-band ESR resonance.[3]

In summary, for a Kondo impurity an ESR resonance can only be observed if T_K is very small. Otherwise the resonance width is going to be too broad to be seen. One possible way to overcome this is to measure in rather high magnetic fields with a correspondingly larger frequency of the electromagnetic field. The above considerations lead to the commonly accepted statement that ESR of a Kondo ion cannot be observed.

C. Paramagnetic Kondo lattice

For the Kondo lattice, in addition to the single site terms, we now consider the multi-site terms in Eq. (12). To second order in J we have for the inter-site terms, i.e. for $i \neq j$, $\langle S_i^z S_j^z\rangle \approx \langle S^z\rangle^2$ and $\langle S_i^+ S_j^-\rangle \approx \langle S_i^+\rangle\langle S_j^-\rangle \approx 0$. The imaginary part of the relaxation function is then

$$\begin{aligned} N^{T''}(\omega \to 0) &= \frac{\pi}{4}(g_f\mu_B J\rho_F)^2\left[\frac{1}{2} + \frac{g_f\mu_B B'/T}{\sinh(g_f\mu_B B'/T)}\right] \\ &+ \frac{\pi}{8}(g_f\mu_B J\rho_F)^2\Big[\tanh(g_f\mu_B B'/2T)\Big]^2 \sum_{ij,i\neq j} \frac{\sin(k_F R_{ij})^2}{(k_F R_{ij})^2} e^{-R_{ij}/l} \quad , \end{aligned} \tag{20}$$

and the relaxation rate is given by

$$\frac{1}{T_{rel}} = \frac{N^{T''}(\omega \to 0)}{\chi_0^T} \quad , \quad \chi_0^T = \frac{C}{T+\theta} \quad , \tag{21}$$

where C is the Curie constant and $\theta \propto T_K$ the Curie-Weiss temperature. The proportionality constant is slightly larger than one.

The two terms of $N^{T''}$ behave differently as a function of $g_f\mu_B B'/T$. For large $g_f\mu_B B'/T$ the single site term decreases by 50% of its zero-field value, while the inter-site term increases

from zero. It now depends on the value of the spin mean-free path l on how many sites are involved and hence which term dominates. In any case $N^{T''}(0)$ is finite (and positive) and consequently $1/T_{rel} \propto T_K$ at low T. The resonance line is then too broad to be observed for the same reason as in the Kondo impurity case discussed above, unless the heavy fermion band is extremely narrow with an effective mass of $10^5 m_e$, where m_e is the free electron mass. For $T \gg T_K$, on the other hand we recover a Korringa-like behavior with a renormalized Korringa constant $(1/(T_{rel}T))$.

D. Kondo lattice with antiferromagnetic order

For simplicity we assume that the antiferromagnetic order consists of a Néel state with two sublattices, so that nearest neighbor spins have opposite ordered magnetic moments. The single site results are the same ones as for the paramagnetic phase, while for the inter-site terms to second order in J we obtain $\langle S_i^z S_j^z \rangle \approx (-1)^{i-j} \langle S^z \rangle^2$, where $i-j$ is either even or odd, giving rise to a sign oscillation. At low T the term $\langle S_i^+ S_j^- \rangle$ is zero if we neglect collective modes. If we include spin waves this expression gives rise to a positive contribution. Without considering collective modes we have, similarly to the paramagnetic case

$$\begin{aligned} N^{T''}(\omega \to 0) &= \frac{\pi}{4}(g_f \mu_B J \rho_F)^2 \left[\frac{1}{2} + \frac{g_f \mu_B B'/T}{\sinh(g_f \mu_B B'/T)} \right] \\ &+ \frac{\pi}{8}(g_f \mu_B J \rho_F)^2 \Big[\tanh(g_f \mu_B B'/2T) \Big]^2 \sum_{ij, i \neq j} (-1)^{i-j} \frac{\sin(k_F R_{ij})^2}{(k_F R_{ij})^2} e^{-R_{ij}/l} \end{aligned} \quad (22)$$

and $N^{T''}$ in an antiferromagnet is reduced as compared to the paramagnet.

In a heavy fermion compound the rare earth spins are usually antiferromagnetically correlated, even if the system does not undergo a phase transition to long-range order. The correlations have short-range character and the susceptibility follows a Curie-Weiss law with antiferromagnetic Weiss-temperature θ_{AF}, $\chi_0 = C/(T + \theta_{AF})$. Here θ_{AF} is determined by the Néel temperature, T_N, the frustration in the system (enhancing θ_{AF}) and T_K. The relaxation rate is

$$\frac{1}{T_{rel}} = \frac{N^{T''}(\omega \to 0)}{\chi_0^T} \ , \quad (23)$$

so that the linewidth roughly follows a Korringa law, with a residual $T = 0$ linewidth proportional to θ_{AF}. Since θ_{AF} is still considerable, the same conclusions as for the paramagnetic phase hold, and a resonance line can only be observed if θ_{AF} is very small.

E. Kondo lattice with ferromagnetic order

On the other hand, if the rare earth spins are ferromagnetically correlated the single site results are the same ones as for the paramagnetic phase, while for the inter-site terms we have $\langle S_i^z S_j^z \rangle \approx \langle S^z \rangle^2$ and $\langle S_i^+ S_j^- \rangle$ is again zero if we neglect collective modes. However, if collective modes such as magnons are considered then these terms yield a positive contribution. The static susceptibility in this case is given by $\chi_0^T = C/(T - T_C)$ for $T > T_C$, where $T_C > 0$ is the Curie temperature. As $T \to T_C$ the susceptibility diverges and, according to expression (23), the ESR linewidth becomes very narrow, and hence observable (see Fig. 2). In general, close to the critical point, we would have to approximate by $\chi_0^T \sim |t|^{-\gamma}$, where $t = (T - T_C)/T_C$ is the reduced temperature and γ is the corresponding critical exponent, which is larger than 1. Hence, the narrowing of the line proceeds even faster as $t \to 0$. This result has to be regarded with caution, because in $N^{T''}$ we have neglected the relaxation through magnons.

If the ferromagnetic correlations are not strong enough to produce long-range order at any temperature, i.e. their nature is short-ranged, then the susceptibility is proportional to $T^{-\gamma}$ and again the relaxation rate is strongly reduced at low T. In this case relaxation through magnons would not play a relevant role, because low energy excitations have a wavelength larger than the range of the correlations. Shorter wavelength magnons cannot be excited because their energy is larger than that of the thermal bath. Hence, there is the possibility that the electron spin resonance can be observed.

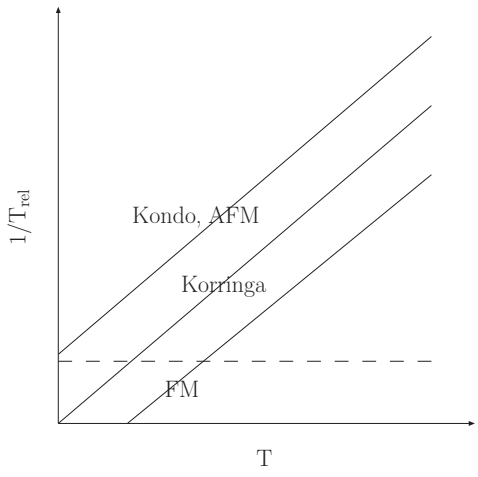

FIG. 2: Sketch of the relaxation rate as a function of T for AFM or Kondo correlations, FM fluctuations and no interactions (Korringa). Close to a magnetic transition (either AFM or FM) there are additional relaxation mechanisms due to collective excitations (spin-waves or magnons) which have not been taken into account here. The horizontal dashed line schematically indicates the resonance energy. Only below that line is a signal observable.

For $YbRh_2Si_2$ the ferromagnetic correlations are predominantly in the *ab*-plane. The linewidth should then depend on whether the field is in the plane or along the c-axis. Hence,

Preprints (www.preprints.org) | NOT PEER-REVIEWED | Posted: 3 May 2018 doi:10.20944/preprints201805.0071.v1

Peer-reviewed version available at Magnetochemistry 2018, 4, 27; doi:10.3390/magnetochemistry4020027

for a field in the ab-plane the short-range ordered domains tend to align, giving rise to a large static susceptibility along the field direction, χ_0^T. In the case of a field oriented along the c-axis, the spins are tilted out of the plane, which should give rise to smaller susceptibilities. The resonance linewidth is then expected to be narrower for the field in the ab-plane, in agreement with the experimental observations.[6,19] Since the in-plane value of the g-factor is much smaller than the one along the c-axis, there is also a magnetic field broadening of the resonance (see Eq. (18)), in addition to the above-mentioned broadening effect.

F. Summary

For the Kondo lattice, the short-range correlations among the localized spins play a fundamental role. If the spins are antiferromagnetically correlated the linewidth is of the order of the Curie-Weiss temperature of the susceptibility. Usually θ_{AF} is too large for ESR to be observed. On the other hand, if the spins are ferromagnetically correlated the linewidth is strongly suppressed and there is the possibility of an ESR signal. In this case the ferromagnetic short-range correlations prevent the spin-flip from being passed on to other sites. To some degree this situation can be interpreted a narrowing of the signal due to bottleneck.[6]

IV. ANTIFERROQUADRUPOLAR ORDERED CEB_6

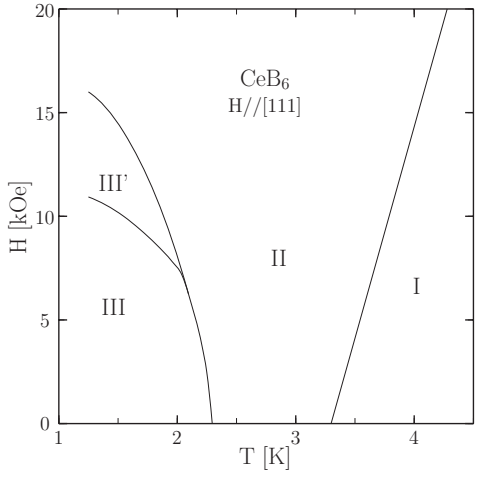

FIG. 3: The low temperature H vs. T phase diagram for CeB_6 displays four phases. Phase I is the paramagnetic Kondo phase. Before the Kondo effect can compensate the internal degrees of freedom there is a second order transition to the antiferro-quadrupolar phase (II) with the Q_{AFQ} at the R point of the Brillouin zone. At lower T in the phases III and III' antiferromagnetism kicks in. Phase diagram taken from Ref. 35.

In contrast to the other compounds discussed above, which have tetragonal symmetry and strong anisotropy, CeB_6 is a cubic crystal. The crystalline field of an eightfold coordination splits the $J = 5/2$ into a Γ_8 ground state quartet and an excited Γ_7 doublet. The crystalline field excitation energy is 540 K, so that for all practical purposes we can ignore the Γ_7.[33,34] The Γ_8 quartet has simultaneously spin and quadrupolar content, which gives rise to a rich phase diagram consisting of four phases, as shown in Fig. 3. The high temperature phase is the paramagnetic Kondo-like state (phase I) above $T_Q = 3.3$ K. The Kondo temperature is approximately 3K. Phase II corresponds to antiferro-quadrupolar order with $Q_{AFQ} = R[\frac{1}{2}, \frac{1}{2}, \frac{1}{2}]$ in the temperature range between $T_N = 2.3$ K and T_Q (assuming zero magnetic field). Below T_N the phase diagram displays two antiferromagnetic phases, phase III with $Q_{AFM,1} = \Sigma[\frac{1}{4}, \frac{1}{4}, 0]$ and as a function of field at $H \approx 1.2$ T phase III' with $Q_{AFM,2} = S[\frac{1}{4}, \frac{1}{4}, \frac{1}{2}]$. In this paper we mainly refer to phase II.

A. g-factor for ESR in phase II of CeB_6

There are numerous examples of ESR studies of systems with Γ_8 ground quartets, e.g. Dy^{3+} ions in the insulator[36] CaF_2 and the metal[37] Au, and Er^{3+} in the heavy fermion low carrier compound YbBiPt.[38] Dy^{3+} and Er^{3+} ions, have large total angular momenta of $J = 15/2$, and in cubic symmetry the splittings require two crystalline field parameters, B_4 and B_6. The energy levels and the wave functions are then not universal, but depend on the ratio B_4/B_6.[39] In contrast, Ce^{3+} ions ($J = 5/2$) only need one parameter, B_4. The wave functions of the Γ_8 ground quartet can be expressed in terms of the J_z eigenstates[39]

$$\begin{aligned} |+\uparrow\rangle &= \sqrt{\tfrac{5}{6}}|+\tfrac{5}{2}\rangle + \sqrt{\tfrac{1}{6}}|-\tfrac{3}{2}\rangle \ , \\ |+\downarrow\rangle &= \sqrt{\tfrac{5}{6}}|-\tfrac{5}{2}\rangle + \sqrt{\tfrac{1}{6}}|+\tfrac{3}{2}\rangle \ , \\ |-\uparrow\rangle &= |+\tfrac{1}{2}\rangle \ , \quad |-\downarrow\rangle = |-\tfrac{1}{2}\rangle \ . \end{aligned} \tag{24}$$

Here $\uparrow$ and $\downarrow$ refer to the spin σ and $+$ and $-$ to the quadrupolar (orbital) degrees of freedom. In ESR experiments it is customary to rotate the magnetic field in the $(1, -1, 0)$ plane. The magnetic field can then be parametrized as $\vec{H} = H(\sin\theta, \sin\theta, \sqrt{2}\cos\theta)/\sqrt{2}$, so that for $\theta = 0$ the field is along the $[0, 0, 1]$-axis, if $\theta = \pi/2$ $\vec{H} \parallel [1, 1, 0]$, and for $\theta = \arctan(\sqrt{2}) = 54.7^o$ the magnetic field points into the $[1, 1, 1]$ direction. The theoretical positions of the resonances strongly depend on the angle θ. There are then six possible

Preprints (www.preprints.org) | NOT PEER-REVIEWED | Posted: 3 May 2018 doi:10.20944/preprints201805.0071.v1

Peer-reviewed version available at Magnetochemistry 2018, 4, 27; doi:10.3390/magnetochemistry4020027

microwave transitions within the quartet, however, two are doubly degenerate, so there are actually only four lines.[40]

Experimentally, however, only *one* ESR signal was observed at 60 GHz in the temperature range from 1.8 to 3.8 K for the field parallel to the [110] direction,[41,42] rather than the four expected lines. The resonance[43] has a Dysonian-like lineshape, characteristic of a metallic environment, and a g-factor of 1.59. The compound displays antiferro-quadrupolar (AFQ) order[44] where the resonance was observed. The long-range order is driven by the quadrupolar degrees of freedom and the $Q_{AFQ} = R[\frac{1}{2},\frac{1}{2},\frac{1}{2}]$ breaks the translational invariance of the lattice, so that there are two interpenetrating sublattices. The problem is conveniently studied within the framework of the Anderson lattice which leads to hybridized localized and conduction states.[40] Within the reduced Brillouin zone there are now twice as many bands, i.e. four, and we need to place four electrons into these bands. The f-electron energies for the two sublattices due to the AFQ order are ε_1 and ε_2 and the corresponding g-factors g_1 and g_2 (they depend also on the direction of the applied field). Within the mean-field slave-boson formulation this leads to a 4×4-matrix Hamiltonian for each $\mathbf{k}$-value, with the single site energies in the diagonal and the hybridization terms on the off-diagonal entries. The diagonalization of the Hamiltonian yields the band dispersions.[40] For heavy fermions, the Fermi level intersects the lower hybridized band close to the band-gap, leading to *one* resonance with effective g-factor $g_{eff} = (g_1+g_2)/2$. This result depends on two angles, namely, the angle θ of the magnetic field with the crystal axis and an angle φ defining the AFQ long-range order.[40]

The magnetization operators only depend on τ_x and τ_z. To define a general direction of the orbital order, it is then natural to rotate the τ-matrices in the x-z plane, i.e.,[40]

$$\tilde{\tau}_x = \cos(\varphi)\tau_x - \sin(\varphi)\tau_z \quad , \quad \tilde{\tau}_z = \sin(\varphi)\tau_x + \cos(\varphi)\tau_z \quad . \tag{25}$$

Without loss of generality we can now choose the quadrupolar order along $\tilde{\tau}_z$. The effective g-factor was found to be[46]

$$\begin{aligned} g_{eff}(\theta,\varphi) \;=\; & \left\{\cos^2(\theta)\left(1+\frac{4}{7}\cos(\varphi)\right)^2 + \sin^2(\theta)\left[\left(1-\frac{2}{7}\cos(\varphi)\right)^2 + \frac{12}{49}\sin^2(\varphi)\right]\right\}^{1/2} \\ & + \left\{\cos^2(\theta)\left(1-\frac{4}{7}\cos(\varphi)\right)^2 + \sin^2(\theta)\left[\left(1+\frac{2}{7}\cos(\varphi)\right)^2 + \frac{12}{49}\sin^2(\varphi)\right]\right\}^{1/2} \\ & - K + \text{corr} \;, \end{aligned} \tag{26}$$

where "corr" is a small negative correction term of the order of 1 to 2 % due to the Zeeman splitting of the conduction electrons and the dispersions of the bands (see Ref. 40). Here $K > 0$ is the "Knight-shift" correction arising from the Hartree-Fock term of the exchange interaction (see Eq. (2)). The magnitude of the Knight-shift correction can be estimated from the Kondo temperature and is expected to be of the order of 0.15 to 0.20% of g_{eff}.

The angular dependence of the resonance at 60 GHz has recently be measured in Ref. 45. Their data with error bars for 1.8 K (open circles) and 2.65 K (dark circles) are shown in Fig. 4. The solid curve is our fit to the data for 2.65 K using Eq. (26) with $\varphi = 0.18\pi$ and $K^* = K - \text{corr} = 0.48$. The constant shift K^* is slightly larger than expected from our simple considerations. This fit is quite different from the one attempted in Ref. 45 and would change their conclusions. All data are taken in the AFQ phase II. For 2.65 K the system is in phase II for all fields, while for 1.8 K the resonance positions vary between 2.4 T and 2.7 T, i.e. not far away from boundary with phase III'. In this region antiferromagnetic spin fluctuations are expected, and the present theory is no longer applicable without caution. Note that a pure AFQ in the absence of field is a "hidden" order phase and cannot be observed by inelastic neutron scattering.

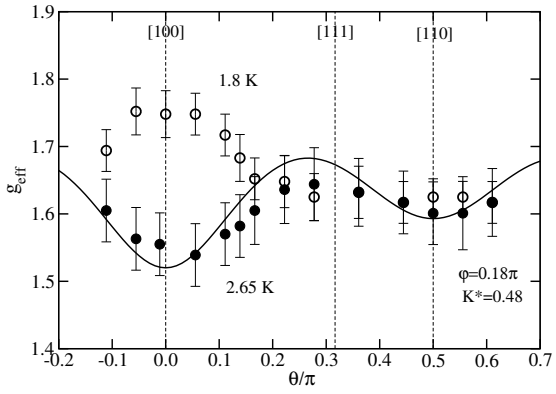

FIG. 4: g_{eff} as a function of θ for the rotation of the magnetic field in the $< 011 >$ plane for two temperatures ($T = 1.8$ K and 2.65 K) from Ref. 45. The solid curve is the fit to theory[40,46] for $T = 2.65$ with $\varphi = 0.18\pi$ and $K^* = 0.48$. Stronger antiferromagnetic fluctuations are expected at 1.8 K.

The fact that only one resonance is observed and the single-ion picture yields two lines, one for each sublattice, shows that the signal in CeB_6 can only be interpreted within the itinerant electron picture. This is in contrast to the compounds discussed in sect. III, which allow an analysis as a single-site or a collective resonance. CeB_6 clearly shows that ESR in heavy fermion systems is a collective phenomenon.

B. Ferromagnetic correlations in phase II of CeB_6

In sect. III we argued that the line width of the resonance is of the order of T_K and too broad to be observed, unless there are ferromagnetic correlations among the moments. The compounds mentioned in sect. III are tetragonal and this anisotropy favors ferromagnetic correlations with the moments oriented in the ab-plane. The isotropy of the cubic CeB_6 lattice is not favorable for ferromagnetic correlations. Ferromagnetic fluctuations have to suppress the Curie-Weiss temperature arising from the Kondo effect or the heavy fermion band. Below we present arguments on how ferromagnetic spin correlations can arise in CeB_6 and render an observable ESR signal in the AFQ ordered phase.

Consider the wave function for two f-electrons on neighboring sites. Each state consists of the product of a coordinate wave function, an orbital (quadrupolar) wave function and a spin wave function[40,46]

$$\Psi \sim \psi_{coor}(\vec{r}_1, \vec{r}_2)\psi_{orb}(m_1, m_2)\psi_{spin}(\sigma_1, \sigma_2) \ . \tag{27}$$

Since these are fermions the total wave function Ψ should be antisymmetric under the interchange of the indices 1 and 2. This implies that either one of the three factors in Eq. (27) is antisymmetric (and the other two symmetric) or all three factors have to be antisymmetric. Since there is no charge density wave, the wave function ψ_{coor} is the product of single site wave functions, $\varphi(\vec{r}_1)\varphi(\vec{r}_2)$, where both electrons are in the same ground state. $\psi_{coor}(\vec{r}_1, \vec{r}_2)$ is then necessarily a symmetric function. Hence, out of $\psi_{orb}(m_1, m_2)$ and $\psi_{spin}(\sigma_1, \sigma_2)$ one has to be antisymmetric and the other one symmetric. We now assume that the effective two-particle interaction Hamiltonian is of the form $\mathcal{H}_{int} = a\vec{\tau}_1 \cdot \vec{\tau}_2$, where a is the quadrupolar exchange. To be able to generate AFQ order necessarily a has to be positive. Hence, $\psi_{orb}(m_1, m_2)$ represents an orbital singlet and has odd parity. Consequently, the spin wave function has to be a triplet (even parity) and the spins are then ferromagnetically correlated.

The singlet state of the quadrupolar degrees of freedom cannot be satisfied simultaneously between all the neighboring sites and generates a resonant valence bond lattice for the quadrupolar wave function. A magnetic field helps to align the spins and hence to enforce the antiferro-orbital correlations. Hence, the magnetic field stabilizes the orbital order. Consequently, the T_c of the phase boundary between the para-quadrupolar disordered (Kondo) phase I and the AFQ phase II increases with magnetic field, as shown in Fig. 3. It is interesting to notice that the rate of increase of T_c with field decreases at higher fields,[47,48] but

Preprints (www.preprints.org) | NOT PEER-REVIEWED | Posted: 3 May 2018 doi:10.20944/preprints201805.0071.v1

Peer-reviewed version available at Magnetochemistry 2018, 4, 27; doi:10.3390/magnetochemistry4020027

does not saturate up to 35 T. This reduced increment of T_c with field is due to the orbital resonant valence bond lattice, which cannot satisfy all bonds simultaneously.

The magnetization shows a sizeable increase in phase II, with a marked increase in slope at the boundary T_c. Hence, the magnetic susceptibility increases quite dramatically, as a consequence of a reduction of the Weiss temperature. In phase I the Weiss temperature θ is of the order of T_K, and in phase II it appears to have changed sign, i.e. the correlations are clearly ferromagnetic[43] (see also Fig. 1 of Ref. 49 and Fig. 5 of Ref. 50). Since the relaxation rate is inversely proportional to the static transversal susceptibility (see Eq. (23)), an enhanced χ_0^T reduces the linewidth and the ESR signal becomes observable. A similar conclusion, although with different arguments, has been presented in Refs. 43 and 45.

Quadrupolar degrees of freedom play a fundamental role in Ce^{3+} and Nd^{3+} ions with Γ_8 ground-state.[51] They manifest themselves in first place through interactions among the sites. There is, however, no consensus about the origin of the interactions. Kubo and Kuramoto[52] successfully described the excitation spectrum of NdB_6 using nearest-neighbour intersite exchange and quadrupolar interactions. A different approach emphasizing crystalline fields was proposed by Uimin and Brenig.[53] For CeB_6, on the other hand, quadrupolar interactions between sites,[54] the RKKY interaction arising from the Coqblin-Schrieffer model,[55,56] and a detailed group theoretical study[57] have been presented.

C. Line width of ESR in phase II of CeB_6

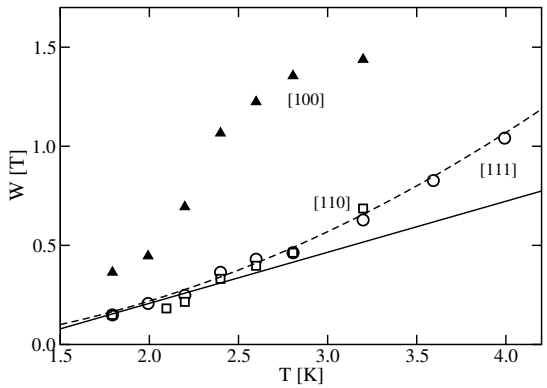

FIG. 5: Line width W of CeB_6 as a function of temperature for the three principal axis from Ref. 45: The dark triangles correspond to [100], the open squares to [110] and the open circles to [111]. The straight line represents a Korringa relaxation for intermediate T and the [110] and [111] directions. The dashed line is a parabolic fit.

The T-dependence of the line width of the Dysonian resonance for the three principal crystallographic directions (data from Ref. 45) is shown in Fig. 5. The solid straight line

corresponds to a Korringa relaxation for a small interval at intermediate T. The figure clearly shows that $1/T_{rel}$ does not have a Korringa-like T-dependence, but a more complicated one. In sect. III we argued that $1/T_{rel}$ is inversely proportional to the susceptibility. It is $1/\chi_0^T$ that provides the dominant T-dependence for $1/T_{rel}$. We can conclude that the susceptibility is smaller in the [100]-direction than in the other two main directions. The anomalous $\chi_0^T(T)$-dependence is due to magnetic fluctuations in phase II for sufficiently large fields, e.g. the difference between the straight line (Korringa) and the dashed curve. At the highest temperature the slight increase of the relaxation rate could also be the beginning of the onset of the Orbach spin-lattice relaxation mechanism[58] into the excited crystalline field Γ_7 doublet.

The g-shift (Knight-shift) for larger fields is proportional to the susceptibility of the conduction states. Hence, the Knight-shift subtraction along the [100]-direction is expected to be smaller for this orientation and consequently g_{eff} is larger at lower T as seen in Fig. 4.

D. Second resonance at high fields in phase II of CeB_6

So far we only considered resonances between the initial and final states belonging to the AFQ condensate in phase II, i.e. both states belong to the ordered phase. At high resonance frequencies, however, the final state of the transition may be outside the energy range of the ordered phase and corresponds to the Kondo phase I. As argued in sect. III the number of final states is larger in the paramagnetic phase I, since all states of the Γ_8 are in principle available and a second (and perhaps third) transition may arise. Assuming a mean-field BCS-type order parameter, the energy of the condensate of the AFQ order is approximately $\Delta = 1.75 \times k_B T_c$. With $T_c \approx 6$ K at the relevant fields, we have $\Delta \approx 10$ K ≈ 200 GHz. Hence, for frequencies less than 200 GHz the initial and the final states of the transition have to belong to the ordered phase and only one transition will be observed. On the other hand, for frequencies larger than 200 GHz the initial (ground) state is in the condensate, while the final (excited) state has to be a free ion (Γ_8) state.

A second resonance was detected by Demishev *et al.*[59] in ESR of CeB_6 for the field in the [110] crystallographic direction for frequencies exceeding 200 GHz. The g-factor of the secondary resonance is considerably smaller than that of the primary line. The intensity

Preprints (www.preprints.org) | NOT PEER-REVIEWED | Posted: 3 May 2018 doi:10.20944/preprints201805.0071.v1

Peer-reviewed version available at Magnetochemistry 2018, 4, 27; doi:10.3390/magnetochemistry4020027

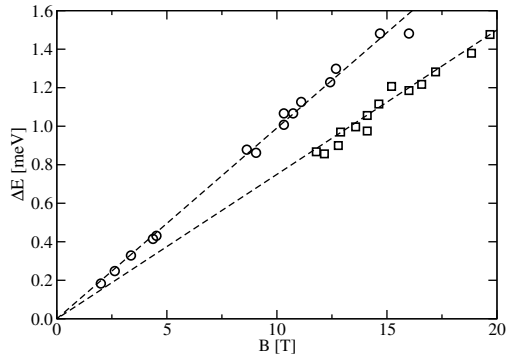

FIG. 6: Magnetic field dependence of the two resonances. One is observed for all fields (open circles) and the other one (open squares) is only seen at high magnetic fields above 12 T.[59] The dashed straight lines correspond to a pure Zeeman splitting with $g_{eff} \approx 1.7$ and $g_{eff} \approx 1.3$, respectively. Data reproduced from Ref. 60.

of the secondary line is also less than that of the primary resonance. The two resonance energies are shown in Fig. 6 as a function of magnetic field (figure adapted from Ref. 60). The splitting is approximately linear in field indicating that it is a Zeeman splitting. In Ref. 59 (Fig. 4) the g-values are plotted as a function of frequency showing a small field-dependence. A calculation of these resonances is rather complicated since the AFQ-ordered state, the Γ_8-states and the coherence of the Anderson lattice needs to be invoked.

E. Inelastic neutron scattering in CeB_6

The ESR results for CeB_6 are complementary and closely related to those of inelastic neutron scattering (INS). While standard ESR measures the transversal dynamical magnetic susceptibility for $\vec{q} = 0$, INS realizes the longitudinal dynamical magnetic susceptibility (see next section) as a function of wave vector $\vec{q}$ and frequency ω. In the paramagnetic Kondo phase, the dynamical susceptibility has a quasi-elastic peak (centered at $\omega = 0$) of width $1/T_1$ given by the maximum of T and T_K. In phase II at zero-field the neutrons do not couple to the ordered quadrupolar moments. This phase is frequently called a "hidden" order phase with $Q_{AFQ} = R[\frac{1}{2}, \frac{1}{2}, \frac{1}{2}]$. A finite magnetic field breaks the symmetry and induces magnetic moments which can be detected by neutrons. Phase III has antiferromagnetic long-range order with $Q_{AFM_1} = \Sigma[\frac{1}{4}, \frac{1}{4}, 0]$ and in phase III' the Q-vector changes to $Q_{AFQ_2} = S[\frac{1}{4}, \frac{1}{4}, \frac{1}{2}]$. The phase diagram is shown in Fig. 3.

There are four types of excitations observed by INS.

1) A **resonant magnetic exciton mode**,[62] similar to the ones found in unconventional superconductors,[63] including heavy fermion superconductors ($CeCu_2Si_2$, $CeCoIn_5$,

Preprints (www.preprints.org) | NOT PEER-REVIEWED | Posted: 3 May 2018 doi:10.20944/preprints201805.0071.v1

Peer-reviewed version available at Magnetochemistry 2018, 4, 27; doi:10.3390/magnetochemistry4020027

$CeRu_2Al_{10}$),[64,65] was observed at $R[\frac{1}{2},\frac{1}{2},\frac{1}{2}]$, but in phase III. The mode is non-dispersive, sharply peaked and associated with the opening of a spin-gap at low energies. The spin-gap is the consequence of the magnetic order, since for $T > T_N$ the resonance peak shifts to $\omega = 0$ and becomes the quasi-elastic peak of the paramagnetic state. A theoretical interpretation of the resonant exciton mode was provided by Akbari and Thalmeier.[66]

2) A strong **FM soft mode** was observed[67] at the zone center (Γ-point). These ferromagnetic fluctuations are large in phase III but also present (although weak) in phase II. There are, however, no dispersive magnon excitations in the AFQ phase. Just above T_N the magnetic intensity collapses into a broad quasi-elastic peak (centered at zero energy). The line width is smallest at the Γ-point. The ferromagnetic fluctuations are expected to be enhanced in a magnetic field and the reason for an accessible ESR signal in CeB_6.

3) **Spin-wave modes** emanate from the AFM wave-vectors Q_{AFM_1} and Q_{AFM_2} below T_N. They display a spin-gap of about 0.3 to 0.4 meV and reach up to 0.7 meV at the zone boundary (M point). Hence, the band width is comparable to the spin-gap. All the above excitations hybridize to form a continuous dispersive magnon band in a narrow energy range. The band is more dispersive in the AFQ phase.

4) In unconventional superconductors a strong magnetic field splits the resonant magnetic exciton mode into two components. This is not the case for CeB_6, where a second field-induced magnon mode emerges whose energy increases with magnetic field.[60] At the FM zone center (Γ-point) only a single mode is found with a non-monotonic field dependence in phase III. Inside the hidden order phase it agrees well with the ESR resonance energy (Fig. 6). INS measurements in the field range of the second (high-field) ESR resonance have not been carried out. It is interesting to point out that this secondary ISN response occurs also at the R-point, which is not accessible by ESR.

INS and ESR results are complementary and there is still much work to be done to understand the magnetic correlations in CeB_6.

F. Summary

In heavy-fermion systems an ESR signal cannot be observed because of antiferromagnetic correlations that broaden the line. There are exceptions in magnetically very anisotropic compounds with ferromagnetic correlations that reduce the line width as discussed in section

III. CeB_6 constitutes an exception to the exceptions, since a resonance was observed in a *cubic* Kondo lattice in the AFQ phase, and needs a separate explanation.

The ground state of each Ce ion is a Γ_8 quartet, displaying spin and orbital degrees of freedom. From the antisymmetry of the electron wave functions we conclude that in order to have AFQ correlations necessarily the spins have to be ferromagnetically coupled at the Γ-point. A magnetic field favors this state and the T_c of the phase boundary between the Kondo phase and the AFQ phase increases with H, in agreement with the experiment. Furthermore, the ferromagnetic correlations enhance the susceptibility (in agreement with experiment where χ_0 displays a kink[43,50]) and hence reduce the line width of the resonance, which then becomes accessible to observation.

Previous ESR experiments on heavy fermion systems with Kramers doublets, e.g. $YbRh_2Si_2$,[4,6–8] have all been interpreted as if the resonance is due to localized f-electrons, i.e. as for ESR on an impurity. The response function in that case is the local dynamical susceptibility, rather than the global dynamical susceptibility.[21,22] However, since more than 60% of the Yb ions participate in the resonance,[19] it is hard to distinguish between the two approaches.[20] The single resonance observed in CeB_6 is evidence (in conjunction with the analysis in Ref. 22) that the ESR signal is a collective phenomenon involving all the sites of the lattice.

Four resonances are expected from a single Ce^{3+} site with a Γ_8 ground quartet. The AFQ order quenches three of these resonances at each site and the coherence in the global susceptibility reduces the signal to one resonance. The experimentally observed g-value[41–43] is about 1.6 and depends on the angle θ of the magnetic field with the crystallographic axis. The theoretical effective g-factor depends on the angle φ of the quadrupolar order in addition to the θ and the Knight shift. There is good agreement between theory and experiment for a proper choice of parameters (in contrast to statements in Ref. 45). The Γ_8 ground state and the antiferro-quadrupolar order are essential ingredients for the observability of an ESR signal in a cubic environment.

V. LONGITUDINAL DYNAMICAL SUSCEPTIBILITY

In a configuration in which the oscillating magnetic field of the microwaves is parallel to the Zeeman field (assumed along the z-axis) the resonance is given by the longitudinal

dynamical susceptibility, $\chi^L(z) = -(g_f\mu_B)^2 \frac{1}{N}\sum_{ij}\langle\langle S_i^z; S_j^z\rangle\rangle_z$. This correlation function, but also as a function of a wave vector $\vec{q}$, contains the response to inelastic neutron scattering (INS). We consider the same Hamiltonian as section II, namely Eq. (1), together with the "Knight"-shifted magnetic field, Eq. (2). To higher order in the Kondo exchange J the model generates a Heisenberg exchange between the different sites (RKKY-interaction). In section III this spin-exchange was incorporated into the expectation values of spin operators and the static susceptibility. The same procedure will be followed here. The longitudinal response for INS consists then of a quasi-elastic central peak of width $1/T_1$ and inelastic peaks arising from the transition (emission and absorption of $\omega(\vec{q})$) into spin-excited states. To study the latter it is convenient to artificially include a Heisenberg Hamiltonian with the appropriate symmetries. Here we limit ourselves to study the quasi-elastic peak.

We apply the equation of motion to the first argument of the susceptibility,[29,30]

$$\begin{aligned} z\langle\langle S_i^z; S_j^z\rangle\rangle_z &= \frac{J}{2N}\sum_{\mathbf{k}\mathbf{k}'\sigma\sigma'} e^{i(\mathbf{k}-\mathbf{k}')\cdot\mathbf{R}_i}\langle\langle (S_i^+ c^\dagger_{\mathbf{k}\sigma} s^-_{\sigma\sigma'} c_{\mathbf{k}'\sigma'} - S_i^- c^\dagger_{\mathbf{k}\sigma} s^+_{\sigma\sigma'} c_{\mathbf{k}'\sigma'}); S_j^z\rangle\rangle_z \\ &= \langle\langle j_i^L; S_j^z\rangle\rangle_z \quad . \end{aligned} \tag{28}$$

The above equation defines the spin-current j_i^L. Applying the equation of motion on the second argument of the correlation function yields

$$z\langle\langle j_i^L; S_j^z\rangle\rangle_z = \langle[j_i^L, S_j^z]\rangle - \langle\langle j_i^L; j_j^L\rangle\rangle_z \quad , \tag{29}$$

which is now evaluated for the noninteracting system.

The Bloch equation can be written into the form[29,30]

$$\chi^L(z) = \left[z + N^L(z)/\chi_0^L\right]^{-1} N^L(z) \quad , \tag{30}$$

where χ_0^L is the static longitudinal magnetic susceptibility and $N^L(z)$ is the longitudinal relaxation function. To second order in the exchange $N^L(z)$ is given by[29,30]

$$\begin{aligned} N^L(z) &\approx -(g_f\mu_B)^2 \frac{1}{N}\sum_{ij} z\langle\langle S_i^z; S_j^z\rangle\rangle_z \\ &= -(g_f\mu_B)^2 \frac{1}{N}\sum_{ij}\frac{1}{z}\left\{\langle\left[j_i^L, S_j^z\right]\rangle - \langle\langle j_i^L; j_j^L\rangle\rangle_z\right\} \quad . \end{aligned} \tag{31}$$

Evaluating the imaginary part of $N^L(z)$ for the noninteracting system we obtain

$$N^{L''}(\omega) = \frac{\pi}{4}(g_f\mu_B J\rho_F)^2\langle S^z\rangle\{2\coth(g_f\mu_B B'/2T) - \frac{\omega + g_f\mu_B B'}{\omega}\coth[(\omega + g_f\mu_B B')/2T]$$

Preprints (www.preprints.org) | NOT PEER-REVIEWED | Posted: 3 May 2018 doi:10.20944/preprints201805.0071.v1

Peer-reviewed version available at Magnetochemistry 2018, 4, 27; doi:10.3390/magnetochemistry4020027

$$+ \frac{\omega - g_f\mu_B B'}{\omega}\coth[(\omega - g_f\mu_B B')/2T]\} + \frac{\pi}{2N}(g_f\mu_B J\rho_F)^2 \sum_{ij,i\neq j} e^{-R_{ij}/l}\frac{\sin(k_F R_{ij})^2}{(k_F R_{ij})^2}$$
$$\times \left[\langle S_i^+ S_j^-\rangle + \langle S_i^- S_j^+\rangle\right] \quad . \tag{32}$$

Here we neglected the Zeeman field of the conduction electrons. The first term is the single site contribution, while the second one arises from the intersite interactions.

We first analyze the single site terms, which correspond to the single impurity case. For $\omega \to 0$ the function $N^{L"}(\omega)$ reduces to

$$N^{L"}(\omega \to 0) = \frac{\pi}{2}(g_f\mu_B J\rho_F)^2\langle S^z\rangle \frac{g_f\mu_B B'/2T}{\sinh^2(g_f\mu_B B'/2T)} \quad . \tag{33}$$

For $g_f\mu_B B' << T$ this expression becomes the constant $(\pi/4)(g_f\mu_B J\rho_F)^2$ and with $\chi_0^L = (g_f\mu_B)^2/4T$ we obtain the Korringa relaxation rate $1/T_1 = \pi(J\rho_F)^2 T$. This is the same expression as for $1/T_2$, since for $g_f\mu_B B' << T$ the dynamical susceptibility is isotropic. In the limit $g_f\mu_B B' >> T$, on the other hand, $N^{L"}(\omega = 0)$ tends to zero exponentially as $\exp(-g_f\mu_B B'/2T)$, because the spin-flips are suppressed by the magnetic field. The suppression of spin-flips also reduces the static susceptibility exponentially, $\chi_0^L = (g_f\mu_B)^2/[4T\cosh^2(g_f\mu_B B'/2T)]$, so that the spin-flip relaxation rate in the high field limit is $1/T_1 = (\pi/2)(J\rho_F)^2 g_f\mu_B B'$, i.e. $T_1 = T_2/2$.[29]

The width of the quasi-elastic central peak is $1/T_1$ and its weight is roughly χ_0^L. In addition to the central peak the longitudinal dynamical response has a shoulder at low T as a function of ω close to $\pm g_f\mu_B B'$. At low T the thermal bath is unable to provide sufficient energy to flip the spin, unless the external frequency is larger than $g_f\mu_B B'$. The Kondo effect is introduced to higher order in J. It affects both the relaxation function $N^L(z)$ and the static susceptibility χ_0^L.[61] Eventually as $T \to 0$ the impurity spin is compensated leading to a finite susceptibility and $1/T_1$ relaxation rate,[31,32] in analogy to the transverse response. The Kondo effect in a small magnetic field smears the abovementioned properties and the characteristic energy of the central peak is the larger of T and T_K. The intersite terms play a substantial role only in the presence of collective excitations, so that expectation values of spin-flips at different sites are nonzero. As for the transversal response function most of the physics is dominated by the static response. Ferromagnetic intersite correlations therefore again narrow the central peak, while AF correlations tend to broaden the quasi-elastic peak.

Peer-reviewed version available at Magnetochemistry 2018, 4, 27; doi:10.3390/magnetochemistry4020027

VI. CONCLUSIONS

An ESR signal for a magnetic impurity in a metal cannot be observed unless the Kondo temperature is very small. This suggests that the line width in heavy-fermion compounds is too broad for measurement with conventional ESR techniques. This common belief was proven incorrect, when an ESR signal was found in several heavy-fermion Ce and Yb systems. Common to these compounds are a strong magnetic anisotropy and ferromagnetic correlations among the rare earth spins, usually in the *ab* plane. The observed resonances have the Dysonian line shape expected for a metallic environment. The ESR relaxation rate is inversely proportional to the static transversal susceptibility. For noninteracting impurities χ_0^T is a Curie law and hence $1/T_2 \propto T$. This is the Korringa relaxation rate, which alternatively can also be obtained from the Fermi-Dirac distribution function of the conduction states.

The Kondo exchange interaction of the resonating spin with the conduction electrons gives rise to the Kondo spin compensation and the susceptibility becomes finite. As a consequence the ESR line width is proportional to T_K and too broad to be observed, unless T_K is much less than the microwave frequency as for Yb impurities in Au.[3] For the Kondo lattice, the short-range correlations among the localized spins play a fundamental role. For heavy fermion compounds, involving Ce^{3+} and Yb^{3+} ions, χ_0^T is inversely proportional to the band width (T_K). If the spins are antiferromagnetically correlated the linewidth is of the order of the Curie-Weiss temperature θ of the susceptibility. θ is usually too large for conventional ESR to be observed. On the other hand, if the spins are ferromagnetically correlated the linewidth is strongly suppressed and there is the possibility of an ESR signal. In this case the ferromagnetic short-range correlations prevent the spin-flip from being passed on to other sites. To some degree this situation can be considered a narrowing of the signal due to bottleneck.[6] The above conclusions for Kondo impurities and the Kondo lattice (i.e., involving localized spins) are similar to those derived for the Anderson impurity and Anderson lattice by Abrahams and Wölfle.[21,22]

The ESR line shape in a metallic environment is Dysonian. This is the case for resonating localized spins,[16] as well as for conduction states.[13–15] For the case of a heavy fermion compound the line shape can then not distinguish between localized spins or conduction states with heavy mass. Similarly from the *g*-values and their anisotropy, we cannot dis-

tinguish between localized and conducting states resonating. For the localized states the g-tensor is determined by the crystalline electric field scheme. Heavy fermions arise from the hybridization of the f-electrons with the conduction states. Close to the Fermi level they are dominated by the f-character and, hence, the g-tensor is predominantly given by the crystalline field scheme of the f-states.

CeB_6 is an exception to the exceptions, since a resonance was observed in a cubic Kondo lattice (no magnetic anisotropy) in the AFQ phase. The ground state of each Ce ion is a Γ_8 quartet, displaying spin and orbital degrees of freedom. Naively, this should give rise to four resonance lines, however only one was observed in the usual range of microwaves. The AFQ long-range order and the coherence of the electron states due to the hybridization are necessary to quench the remaining transitions. The agreement of the angular dependence of the spectrum in the AFQ phase with theory is remarkable. At low T there are differences because of the proximity of phase III, which induces AF correlations not included in the theory. It also follows from the antisymmetry of the electron wave functions that in order to have AFQ correlations necessarily the spins have to be ferromagnetically coupled. A magnetic field favors this state and the T_c of the phase boundary between the Kondo phase and the AFQ phase increases with H, as found experimentally. In addition, the ferromagnetic correlations enhance the magnetic susceptibility[43,50] and hence reduce the ESR line width, which then becomes accessible to observation.

A second resonance was detected[59] in ESR of CeB_6 for frequencies exceeding 200 GHz. The g-factor of the secondary resonance and its intensity are considerably less than that of the primary line. The second resonance can be explained as a transition from the AFQ-ordered resonance into a final state belonging to phase I (Kondo phase).

The INS results for CeB_6 have provided insights about the low T ordered phases and their spin correlations. More work is still needed to relate the INS experiments to the ESR results.

---

[1] K. Yamada, Prog. Theor. Phys. **53**, 970 (1975).

[2] H. Shiba, Prog. Theor. Phys. **54**, 967 (1975).

[3] Y. von Spalden, E. Tsang, K. Baberschke, and P. Schlottmann, Phys. Rev. B **28**, 24 (1983); **29**

487(E) (1984).

[4] J. Sichelschmidt, V.A. Ivan'shin, J. Ferstl, C. Geibel, and F. Steglich, Phys. Rev. Lett. **91**, 156401 (2003).

[5] V.A. Ivan'shin, L.K. Aminov, I.N. Kurkin, J. Sichelschmidt, O. Stockert, J. Ferstl, and C. Geibel, Zh. Eksp. Teor. Fiz. Pis'ma Red. **77**, 625 (2003); [JETP Lett. **77**, 526 (2003)].

[6] J.G.S. Duque, E.M. Bittar, C. Adriano, C. Giles, L.M. Holanda, R. Lora-Serrano, P.G. Pagliuso, C. Rettori, C.A. Pérez, R.W. Wu, C. Petrovic, S. Maquilon, Z. Fisk, D.L. Huber, and S.B. Oseroff, Phys. Rev. B **79**, 035122 (2009).

[7] J. Sichelschmidt, J. Wykhoff, H.-A. Krug von Nidda, I.I. Fazlishanov, Z. Hossain, C. Krellner, C. Geibel, and F. Steglich, J. Phys.: Condens. Matter **19**, 016211 (2007).

[8] C. Krellner, T. Förster, H. Jeevan, C. Geibel, and J. Sichelschmidt, Phys. Rev. Lett. **100**, 066401 (2008).

[9] V.A. Ivan'shin, A.A. Sukhanov, D.A. Sokolov, M.C. Aronson, S. Jia, S.L. Bud'ko, and P.C. Canfield, J. Alloys Compd. **480**, 126 (2009).

[10] E.M. Bruning, C. Krellner, M. Baenitz, A. Jesche, F. Steglich, and C. Geibel, Phys. Rev. Lett. **101**, 117206 (2008).

[11] S.V. Demishev, A.V. Semeno, Yu.B. Paderno, N.Yu. Shitsevalova, and N.E. Sluchanko, Phys. Status Solidi B **242**, R27 (2005).

[12] S.V. Demishev, A.V. Semeno, A.V. Bogach, Yu.B. Paderno, N.Yu. Shitsevalova, and N.E. Sluchanko, J. Magn. Magn. Mater. **300**, e-534 (2006).

[13] G. Feher and A.F. Kip, Phys. Rev. **98**, 337 (1955).

[14] F.J. Dyson, Phys. Rev. **98**, 349 (1955).

[15] G.E. Pake and E.M. Purcell, Phys. Rev. **74**, 1184 (1948).

[16] C. Rettori, D. Davidov, R. Orbach, E.P. Chock, and B. Ricks, Phys. Rev. B **7**, 1 (1973).

[17] C. Rettori, D. Davidov, and H.M. Kim, Phys. Rev. B **8**, 5335 (1973).

[18] C. Rettori, H.M. Kim, E.P. Chock, and D. Davidov, Phys. Rev. B **10**, 1826 (1974).

[19] J. Sichelschmidt, V.A. Ivan'shin, J.Ferstl, C. Geibel, and F. Steglich, J. Magn. Magn. Mater. **272-276**, 42 (2004).

[20] P. Schlottmann, Phys. Rev. B **79**, 045104 (2009).

[21] E. Abrahams and P. Wölfle, Phys. Rev. B **78**, 104423 (2008).

[22] P. Wölfle, and E. Abrahams, Phys. Rev. B **80**, 235112 (2009).

[23] E. Abrahams and P. Wölfle, PNAS **109**, 3238 (2012).

[24] P. Wölfle, and E. Abrahams, Phys. Rev. B **84**, 041101 (2011).

[25] A.A. Zvyagin, V. Kataev, and B. Büchner, Phys. Rev. B **80**, 024412 (2009).

[26] D.L. Huber, J. Phys.: Condens. Matter **21**, 322203 (2009).

[27] B.I. Kochelaev, S.I. Belov, A.M. Skvortsova, A.S. Kutuzov, J. Sichelschmidt, J. Wykhoff, C. Geibel, and F. Steglich, Eur. Phys. J. B **72**, 485 (2009).

[28] F. Bloch, Phys. Rev. **70**, 460 (1946).

[29] W. Götze and P. Wölfle, J. Low Temp. Phys. **5**, 575 (1971).

[30] W. Götze and P. Wölfle, J. Low Temp. Phys. **6**, 455 (1972).

[31] W. Götze and P. Schlottmann, Solid State Commun. **13**, 17 (1973).

[32] W. Götze and P. Schlottmann, J. Low Temp. Phys. **16**, 87 (1974).

[33] T. Fujita, M. Suzuki, T. Komatsubara, S. Kunii, T. Kasuya, and T. Ohtsuka, Solid State Commun. **35**, 569 (1980).

[34] E. Zirngiebl, B. Hillebrands, S. Blumenröder, G. Güntherodt, M. Loewenhaupt, J.M. Carpenter, K. Winzer, and Z. Fisk, Phys. Rev. B **30**, 4052 (1984).

[35] K. Kunimori, M. Kotani, H. Funaki, H. Tanida, M. Sera, T. Matsumura, and F. Iga, J. Phys. Soc. Jpn. **80**, SA056 (2011).

[36] R.W. Bierig and M.J. Weber, Phys. Rev. **132**, 164 (1963).

[37] D. Davidov, R. Orbach, C. Rettori, L.J. Tao, and E.P. Chock, Phys. Rev. Lett. **28**, 490 (1972).

[38] G.B. Martins, D. Rao, G.E. Barberis, C. Rettori, R.J. Duro, J. Sarrao, Z. Fisk, S. Oseroff, and J.D. Thompson, Phys. Rev. B **52**, 15062 (1995).

[39] K.R. Lea, M.J.M. Leask, and W.P. Wolf, J. Phys. Chem. Solids **23**, 1381 (1962).

[40] P. Schlottmann, Phys. Rev. B **86**, 075135 (2012).

[41] S.V. Demishev, A.V. Semeno, Yu.B. Paderno, N.Yu. Shitsevalova, and N.E. Sluchanko, Phys. Stat. Sol. (b) **242**, R27 (2005).

[42] S.V. Demishev, A.V. Semeno, A.V. Bogach, Yu.B. Paderno, N. Yu. Shitsevalova, and N.E. Sluchanko, J. Magn. Magn. Mater. **300**, e-534 (2006).

[43] S.V. Demishev, A.V. Semeno, A.V. Bogach, N.A. Samarin, T.V. Ishchenko, V.B. Filipov, N.Yu. Shitsevalova, and N.E. Sluchanko, Phys. Rev. B **80**, 245106 (2009).

[44] J. Effantin, J. Rossat-Mignod, P. Burlet, H. Bartholin, S. Kunii, and T. Kasuya, J. Magn. Magn. Mater. **47-48**, 145 (1985).

[45] A.V. Semeno, M.I. Gilmanov, A.V. Bogach, V.N. Krasnorussky, A.N. Samarin, N.A. Samarin, N.E. Sluchanko, N.Yu. Shitsevalova, V.B. Filipov, V.V. Glushkov, and S.V. Demishev, Sci. Rep. **6**, 39196 (2016).

[46] P. Schlottmann, J. Appl. Phys. **113**, 17E109 (2013).

[47] D. Hall, Z. Fisk and R.G. Goodrich, Phys. Rev. B **62**, 84 (2000).

[48] R.G. Goodrich, D.P. Young, D. Hall, L. Balicas, Z. Fisk, N. Harrison, J. Betts, A. Migliori, F.M. Woodward, and J.W. Lynn, Phys. Rev. B **69**, 054415 (2004).

[49] C. Terzioglu, D.A. Browne, R.G. Goodrich, A. Hassan, and Z. Fisk, Phys. Rev. B **63**, 235110 (2001).

[50] C. Terzioglu, O. Ozturk, A. Kilic, R.G. Goodrich, and Z. Fisk, J. Magn. Magn. Mater. **298**, 33 (2006).

[51] J. Stankiewicz, M. Evangelisti, Z. Fisk, P. Schlottmann, and L. Gor'kov, Phys. Rev. Lett. **108**, 257201 (2012).

[52] K. Kubo and Y. Kuramoto, J. Phys.: Condens. Matter **15**, S2251 (2003).

[53] G. Uimin and W. Brenig, Phys. Rev. B **61**, 60 (2000).

[54] G. Uimin, Y. Kuramoto, and N. Fukushima, Solid State Commun. **97**, 595 (1996).

[55] F. J. Ohkawa, J. Phys. Soc. Jpn. **54**, 3909 (1985).

[56] P. Schlottmann, Phys. Rev. B **62**, 10067 (2000).

[57] R. Shiina, H. Shiba, and P. Thalmeier, J. Phys. Soc. Jpn. **66**, 1741 (1997).

[58] R. Orbach, Proc. Royal Soc. A **264**, 458 (1961).

[59] S.V. Demishev, A.V. Semeno, H. Ohta, S. Okubo, Yu.B. Paderno, N.Yu. Shitselova, and N.E. Sluchanko, Appl. Magn. Reson. **35**, 319 (2008).

[60] F.Y. Portnichenko, S.M. Demishev, A.V. Semeno, H. Ohta, A.S. Cameron, M.A. Surmach, H. Jang, G. Friemel, A.V. Dukhnenko, N. Yu. Shitselova, V.B. Filipov, A. Schneidewind, J. Ollivier, A. Podlesnyak, and D.S. Inosov, Phys. Rev. B **94**, 035114 (2016).

[61] W. Götze and P. Schlottmann, J. Low Temp. Phys. **112**, 149 (1973).

[62] G. Friemel, Y. Li, A.V. Dukhnenko, N.Y. Shitselova, N.E. Sluchanko, A. Ivanov, V.B. Filipov, B. Keimer, and D.S. Isonov, Nature Commun. **3**, 830 (2012).

[63] D.S. Inosov, J.T. Park, P. Bourges, D.L. Sun, Y. Sidis, A. Schneidewind, K. Hradil, D. Haug, C.T. Lin, B. Keimer, and V. Hinkov, Nature Phys. **6**, 178 (2010).

[64] C. Stock, C. Broholm, J. Hudis, H.J. Kang, and C. Petrovic, Phys. Rev. Lett. **100**, 087001

(2008).

[65] O. Stockert, J. Arndt, E. Faulhaber, C. Geibel, H. S. Jeevan, S. Kirchner, M. Loewenhaupt, K. Schmalzl, W. Schmidt, Q. Si, and F. Steglich, Nature Phys. **7**, 119124 (2011).

[66] A. Akbari and P. Thalmeier, Phys. Rev. Lett. **108**, 146403 (2012).

[67] H. Jang, G. Friemel, J. Ollivier, A.V. Dukhnenko, N.Yu. Shitselova, V.B. Filipov, B. Keimer, and D.S. Inosov, Nat. Mater. **13**, 682 (2014).